Journal of Harbin Engineering University
ISSN: 1006-7043

Vol 45 No. 6
June 2024

Advanced Classification CT Heart Images Using Second Order PDE Filter and Different Feature Extraction Techniques

K. Somasundaram[1*], R. Sathish Kumar[1], S. Sanjayprabu[1], R. Karthikamani[2]
[1]Sri Ramakrishna Mission Vidyalaya College of Arts and Science, Coimbatore, Tamil Nadu, India.
[2]Sri Ramakrishna Engineering College, Coimbatore, Tamil Nadu, India

Abstract:
This paper presents a comprehensive approach to improving the analysis of heart CT images through advanced image processing techniques. We employ the D2Q9 lattice model for efficient filtration, specifically tailored to solve the Perona-Malik second-order partial differential equation, a nonlinear diffusion model widely utilized in image denoising and edge enhancement. Additionally, we integrate histogram-based local descriptors to extract meaningful features from the processed images, facilitating more accurate characterization of cardiac structures and abnormalities. Furthermore, the KNN Classifiers utilized to optimize the classification of heart CT images based on the extracted features.

Keywords: CT; Perona-Malik Second order differential equation; Nonlinear diffusion equation; KNN classifier

1. Introduction

Heart CT imaging plays a crucial role in the detection of heart blocks, enabling visualization of cardiac anatomy and electrical conduction pathways by accurately identifying structural abnormalities such as atrioventricular blockages [1]. CT scans are valuable for planning cardiac interventions, such as stent placement or bypass surgery. CT scans provide detailed, high-resolution images of the heart and surrounding structures. This level of detail is particularly valuable for assessing coronary artery anatomy, detecting blockages, and evaluating the presence of calcifications or plaques. Speed and Accessibility. Moreover, the burden of heart disease and heart blocks among young people all over the world underscores the importance of preventive strategies, early detection, and access to affordable healthcare services. By providing detailed anatomical information, CT scans help cardiologists and surgeons determine the optimal approach for treatment.

In comparison to electrocardiography (ECG) and magnetic resonance imaging (MRI), heart CT imaging offers superior anatomical visualization and diagnostic accuracy for heart blocks and heart diseases. While ECG primarily assesses electrical activity and MRI provides functional and tissue characterization, CT scans combine high-resolution imaging with rapid acquisition, enabling comprehensive assessment of cardiac structure and function [2].

Conduct a thorough comparison with existing numerical methods for solving the Perona-Malik equation, highlighting the superiority of the proposed Lattice Boltzmann approach in terms of accuracy, efficiency, and applicability [3].

This study explains a computational technique along with differential concepts for diagnosing and classifying Heart Blocks using CT Scan images. First, we apply the second-order partial differential equation (PDE) filter to the pre-processed images. The PDE filter enhances texture features by emphasizing edges and texture boundaries while suppressing noise. Then we propose some Statistical feature Extraction metrics namely, GDP, LGP, LGiP along with KNN Classifier analyse geometrical properties.

The following method is dividing into four stage : procedure for using a second-order partial differential equation (PDE) filter for texture feature extraction, followed by statistical feature extraction (MDP, LGP, LGiP), and classification using a K-nearest neighbours (KNN) classifier and finally analyse the Classifier's performance interms of standard parameters. Here we have given Heart CT images is Shown in Figure 2. The following is the format of the paper Section 1.The imaging Technique Heart disease is described. In Section 2 discuss the collection and preparation of data,

Section 3.Describes Second Order PDE FilterationTechnique. Feature Extraction and its Characteristics in Heart CT images are explained in Section 4.The Observation are taken by the Classifiers are shown in Section 5.The Experimental Results Discussed in Section 6. Finally come to a conclusion in section7.

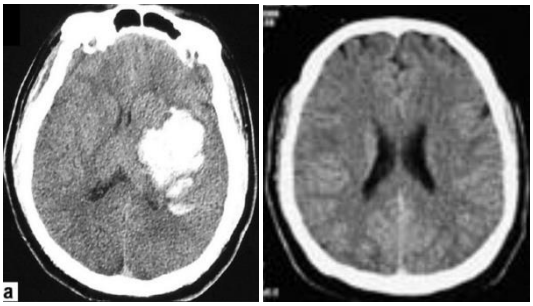

Figure 1. Abnormal CT image vs Normal CT image

Figure 2. Workflow diagram

2. Materials and Methods

2.1. Image Acquisition

The heart CT image dataset was obtained from the open-source Kaggle database. This dataset contains 200 CT scan images, of which 99 are normal and the remaining 101 are abnormal.

2.2. Image Pre-processing

The initial phase of pre-processing is to resize these Heart CT Scan images and choose a suitable filter from the RGB image for the Heart CT image. Heart CT scan images are converted to grayscale from RGB images using the method described below. All resized photos are converted to 256 X 256 pixels. The RGB images are then converted to greyscale for filtering. This task must be completed to increase the image's quality for subsequent processing.

3. Lattice Boltzmann method for Perona Malik Equation

Perona Malik Equation in the form as

$$\frac{\partial r}{\partial t} = \begin{cases} \nabla.(\alpha|\nabla r|\nabla r) \\ r(y,0) = r_0(y) \end{cases} \quad (1)$$

where pixel is taken as y, The intensity of an image at position y and time 't ' is denoted r(y,t) when t=0 , $r_0(y)$ is the intensity of an image at position at y. $\alpha(.)$ is a positive non increasing diffusion coefficient. In Perona and Malik defined two diffusion coefficient $\beta(s) = e^{(-\frac{s}{k})^2}$ and $\beta(s) = \frac{1}{1+(\frac{s}{k})^2}$, where k (threshold value) will be present or altered as image iterates, s is the absolute value of the image gradient$|\nabla u|$. [4]

Using the P-M Equation, a specific convection diffusion equation, we may establish a corresponding D2Q9 model.

The equilibrium distribution function is considered as

$$r_i^{eq} = \alpha_i r(y,t) \quad (2)$$

For D2Q9 model,

$$c_{i=} \begin{cases} (0,0) & \text{i=0} \quad (3) \\ (\cos[(j-1)\frac{\pi}{2}], \sin[(j-1)\frac{\pi}{2}]c & \text{i = 1,2,3,4} \\ (\cos[(j-5)\frac{\pi}{2}+\frac{\pi}{4}], \sin[(j-5)\frac{\pi}{2}+\frac{\pi}{4}])\sqrt{2c} & \text{i = 5,6,7,8} \end{cases}$$

Where $c = \frac{dx}{dt}$, dx is latting space &

$$\alpha_i = \begin{cases} \frac{4}{9} & \text{i=0} \\ \frac{1}{9} & \text{i=1, 2, 3, 4} \\ \frac{1}{36} & \text{i= 5,6,7,8} \end{cases}$$

$\sum_i \alpha_i = 1$ and r(y,t) is defined by

$r(y,t) = \sum_i r_i(y,t)$

Then $\sum_i r_i = \sum_i r_i^{eq} = r$

$\sum_i c_i r_i^{(eq)} = 0$, $\sum_i c_i c_i r_i^{(eq)} = c_s^2 uI.$ (4)

Where $c_s^2 = \frac{c^2}{3}$ for D2Q9 .

We can use the Chapman-Enskog Expansion technique to construct the macroscopic equation (1),

$r_i = r_i^{(0)} + \epsilon r_i^1 + \epsilon^2 r_i^2,$

$\partial_t = \epsilon \partial_{t_1} + \epsilon^2 \partial_{t_2}$ $\nabla = \epsilon \nabla_1$ (5)

Where $r_i^{(0)} = r_i^{(eq)}, \epsilon$ is a small expansion parameter, $t_1 = {}^{t}/_{\epsilon}$ and $t_1 = {}^{t}/_{\epsilon^2}$ (two macroscopic scales)

Taking summation of equation (5) over i

$\sum_i r_i^{(k)} = 0 \ (k \geq 1).$ (6)

Apply Taylor expansion in equation (2), we get

$$D_i r_i + \frac{\Delta t}{2} D_i^2 r_i + \cdots = -\frac{1}{\tau \Delta t}\left(r_i - r_i^{(eq)}\right) \quad (7)$$

Where $D_i = \partial_t + \boldsymbol{c_i}.\nabla$.

Denote $D_{1i} = \partial_{t1} + \boldsymbol{c_i}.\nabla_1$.

Substituting (5) in equation (7),

$$D_{1i} r_i^{(eq)} = -\frac{1}{\tau \Delta t} r_i^{(1)}, \quad (8)$$

$$\partial_{t2} r_i^{(eq)} + D_{1i} r_i^{(1)} + \frac{\Delta t}{2} D_i^2 r_i^{(eq)} = -\frac{1}{\tau \Delta t} r_i^{(2)} \quad (9)$$

Substituting (8) to the left side of (9) and

$$\partial_{t2} r_i^{(eq)} + D_{1i}\left[\left(1 - \frac{1}{2\tau}\right) r_i^{(1)}\right] = -\frac{1}{\tau \Delta t} r_i^{(2)}. \quad (10)$$

Add (8) and (10) over i and using (4) and (6), we obtain $\partial_{t1} r = 0$, (11)

$$\partial_{t2} r + \nabla_1\left[\left(1 - \frac{1}{2\tau}\right)\right] \sum_i c_i r_i^{(1)} = 0 \quad (12)$$

Using (8) and (4) we have $\sum_i c_i r_i^{(1)} = -\tau \Delta t \sum_i c_i D_{1i} r_i^{(eq)}$

$$= -\tau \Delta t c_s^2 \nabla_1 r. \quad (13)$$

So, substituting (13) into (12), we obtain

$$\partial_{t2} r = \nabla_1.\left\{\left[c_s^2\left(\tau - \frac{1}{2}\right)\Delta t\right]\nabla_1 r\right\}. \quad (14)$$

Combining (14) and (11), and taking $\propto = c_s^2\left(\tau - \frac{1}{2}\right)\Delta t$, we have $\partial_t r = \nabla.(\alpha \nabla r)$,

P-M equation is exactly recovered to order $O(\epsilon^2)$.

4. Feature Extraction Techniques

4.1. GDP (Global Distribution of Pixel):

The first step involves computing the gradient of the image to capture the variations in intensity across different regions. This is often achieved using gradient operators such as Sobel, Prewitt, or Scharr filters, which highlight edges and boundaries in the image. the gradient directions are quantized into a predefined number of bins or sectors. This discretization process divides the gradient directions into distinct angular ranges, allowing for the encoding of directional information. For each pixel in the image, a directional pattern is encoded based on the gradient directions in its local neighborhood. This encoding scheme captures the spatial distribution of gradient directions, reflecting the underlying textural properties of the image. Descriptors are computed for each local region of the image based on the encoded directional patterns. These descriptors summarize the distribution of gradient orientations within each region and serve as compact representations of the local texture patterns. The computed descriptors from all local regions are aggregated into a feature vector representation for the entire image. This feature vector encapsulates the global textural characteristics of the image, capturing the arrangement and orientation of texture elements.

Post processing steps, such as normalization or feature selection, may be applied to refine the feature vector and enhance its discriminative power. This could involve techniques like Principal Component Analysis (PCA) to reduce dimensionality or feature scaling to ensure uniformity.

GDP $= \frac{1}{N} \sum_{i=1}^{N-1} I_i$

Where GDP computes the average pixel intensity across the entire image, where I_i represents the intensity value of the i^{th}pixel, and *N* is the total number of pixels in the image [6].

Post processing steps, such as normalization or feature selection, may be applied to refine the feature vector and enhance its discriminative power. This could involve techniques like Principal Component Analysis (PCA) to reduce dimensionality or feature scaling to ensure uniformity.

The extracted feature vectors are utilized in various image processing tasks, such as image classification, segmentation, or content-based retrieval. They serve as the basis for analyzing and interpreting the image content, enabling automated decision-making and understanding in diverse applications.

4.2. LDP (Local Distribution Pattern):

LDP (Local Descriptor Patterns) feature extraction is a fundamental technique in image processing, pivotal for tasks like object recognition, texture analysis, and image retrieval. By encoding local texture patterns through comparisons of pixel intensities in circular neighborhoods, LDP creates compact descriptors capturing essential structural details within localized image regions. These descriptors, aggregated into feature vectors, provide a comprehensive representation of textural characteristics across the entire image, enabling efficient analysis and interpretation. With its ability to extract robust texture information, LDP plays a crucial role in facilitating automated

decision-making and understanding in various image processing applications.

LD$P_k = \frac{1}{n} \sum_{i=0}^{n-1} H_k(i)$

LDP characterizes the distribution of pixel intensities within local regions or patches of an image.$H_k(i)$represents the histogram of pixel intensities within the i^{th}local region [7].

4.3.LDiP (Local Distribution of Intensity Patterns):

LDiP (Local Directional Pattern) feature extraction in image processing is a pivotal method for capturing intricate textural details essential for various tasks like texture classification, object recognition, and content-based image retrieval. By computing gradients and quantizing directional information, LDiP effectively encodes local texture patterns, enabling the creation of compact descriptors summarizing structural features within localized image regions. These descriptors, aggregated into feature vectors, offer a comprehensive representation of global textural characteristics, facilitating accurate analysis and interpretation of image content. LDiP's ability to capture nuanced texture variations empowers automated decision-making and understanding in diverse image processing applications.

LD$iP_k = \frac{1}{n} \sum_{i=0}^{n-1} P_k(i)$

LDiP analyzes the distribution of intensity patterns within local neighborhoods of an image.$P_k(i)$represents the probability distribution of intensity patterns within the i^{th} local neighborhood, and *n* is the total number of local neighborhoods [8].

5. Classification

5.1. K-Nearest Neighbor

The K-Nearest Neighbors (K-NN) classifier stands as a cornerstone in image processing, providing an intuitive yet robust method for classification tasks. Operating on the principle of proximity, K-NN assigns labels to new data points by discerning the majority class among their K nearest neighbors in the feature space. In the context of image processing, where feature extraction is crucial, K-NN utilizes various techniques to represent images effectively. These may include pixel-based representations or more sophisticated feature extraction methods such as Histogram of Oriented Gradients (HOG) or Local Binary Patterns (LBP). Once the features are extracted, distance metrics like Euclidean distance or cosine similarity are applied to measure the similarity between images, allowing K-NN to locate the most similar images in the dataset.

Euclidean distance:$\sqrt{\sum_{i=1}^{n}(x_i - y_i)^2}$

Cosine similarity: $\frac{X \,.Y}{\|X\|\|Y\|}$

Upon determining the K nearest neighbors, K-NN employs a majority voting scheme to assign the label of the new data point, ensuring robust classification outcomes. However, the choice of K and the selection of appropriate features profoundly impact the classifier's performance. Despite its simplicity, K-NN thrives in image processing applications, providing reliable results in tasks such as object recognition, facial recognition, and image retrieval. By leveraging K-NN's adaptability and ease of implementation, practitioners can navigate complex image datasets with confidence, facilitating advancements in various domains of image processing.

For a test datapoint x_i, the K-NN algorithm selects the k nearest neighbors from the training set based on the smallest distance:

$$N_i = \{x_{j_1}, x_{j_2} \ldots\ldots x_{j_k}\}$$

Once the nearest neighbors are identified, the class label ofx_i is determined by the group of class among its knearest neighbors. Let y_{j_m}denote class label of the m-th nearest neighborx_{j_m}. Then y_i computed as

$$y_i = argmax\left(\sum_{m=1}^{k} \delta\,(y_{j_m}, c)\right)$$

Where c represents the possible class labels, and $\delta(.)$ is the Kronecker delta function which returns 1 if its direction are equal and 0. Otherwise the y_i represents the predicted class label corresponding x_i [13].

6. Experimental Results

There are a total of 200 images of the Heart CT image data set that were used to generate the input images. The feature extraction values are fed into the KNN classifier in this experiment. Next, common parameters are used to evaluate the feature approaches' performance. Feature extraction techniques are used to calculate standard parameters such as accuracy, sensitivity,

and specificity. These metrics can be found in Table 2. The standard parameters can be found using the following formulas.

An accurate test can distinguish between patients and healthy cases with high accuracy. The total number of real positive as well as negative cases among each examined case must be computed to assess the accuracy of a test. It is possible to express the same mathematically.

$$\text{Sensitivity} = \frac{\text{TP}}{\text{TP+FN}} * 100$$

$$\text{Specificity} = \frac{\text{TN}}{\text{TN+FP}} * 100$$

$$\text{Accuracy} = \frac{\text{TP+TN}}{\text{TP+TN+FP+FN}} * 100$$

$$\text{Error rate} = \frac{\text{FN+FP}}{\text{TP+TN+FN+FP}} * 100$$

$$\text{Precision} = \frac{\text{TP}}{\text{TP+FP}} * 100$$

$$\text{F1 Score} = \frac{2 * \text{TP}}{(2 * \text{TP}) + \text{FN} + \text{FP}} * 100$$

$$\text{Jacard Metric} = \frac{\text{TP}}{\text{TP} + \text{FN} + \text{FP}} * 100$$

$$\text{BCR} = \frac{\text{Sensitivity} + \text{Specificity}}{2}$$

$$\text{MC} = \frac{(\text{TP} * \text{TN}) - (\text{FP} * \text{FN})}{\sqrt{(\text{TP} + \text{FP}) * (\text{TP} + \text{FN}) * (\text{TN} + \text{FP}) * (\text{TN} + \text{FN})}}$$

Table 1. Confusion matrix for KNN classifier with GDP

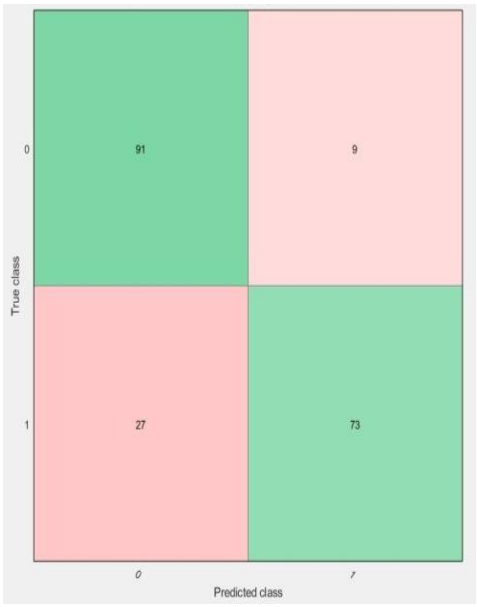

Table 2. Confusion matrix for KNN classifier with LGP

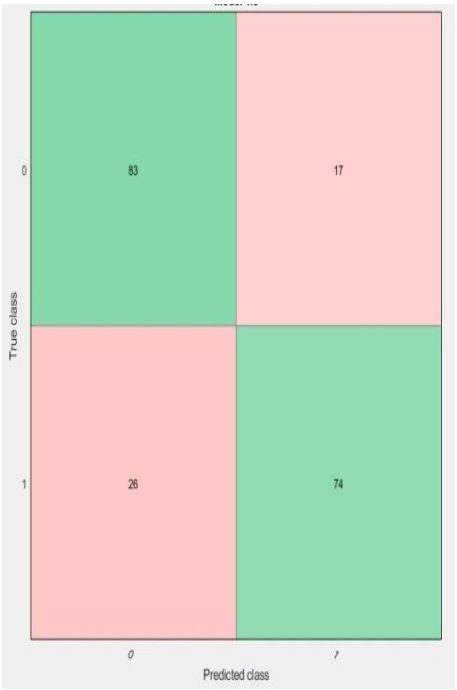

Table3. Confusion matrix for KNN classifier with LGiP

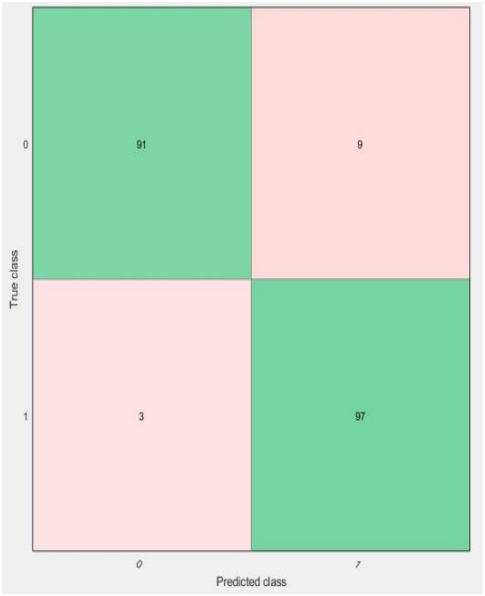

- True Negatives (TN) refer to cases where the model or test correctly identifies individuals as negative, meaning they do not have the condition or illness.
- False Positives (FP) occur when the model or test incorrectly identifies individuals as positive when they do not have the condition or illness (A type of error where healthy individuals are wrongly labeled as suffering).
- False Negatives (FN) happen when the model or test incorrectly identifies individuals as

negative individuals with the illness are mistakenly labeled as healthy).

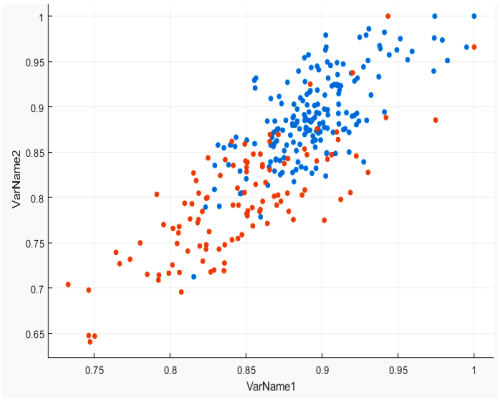

Figure 3. Scatter plot of GDP

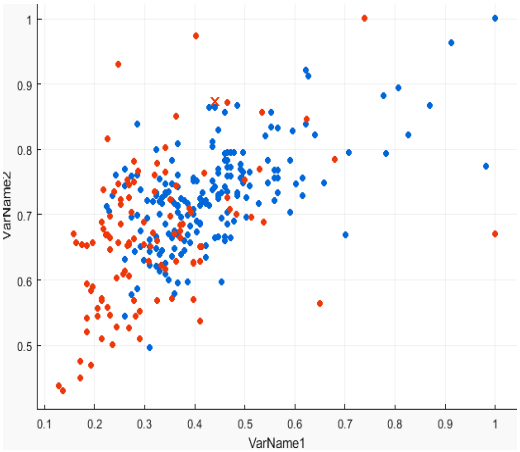

Figure 4. Scatter plot of LGP

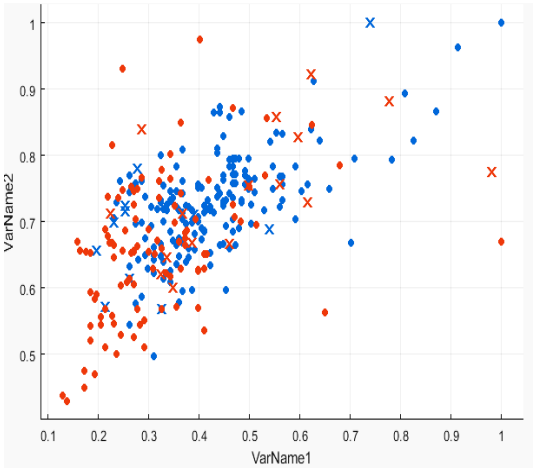

Figure 5. Scatter plot of LGDiP

When they actually have the condition or illness (a type of error) where Figure 3,4 and 5 depicts Scatter Plot GDP, LGP, LGDiP Feature Extraction Techniques. Performance Analysis of KNN Classifier with Feature Extraction Technique

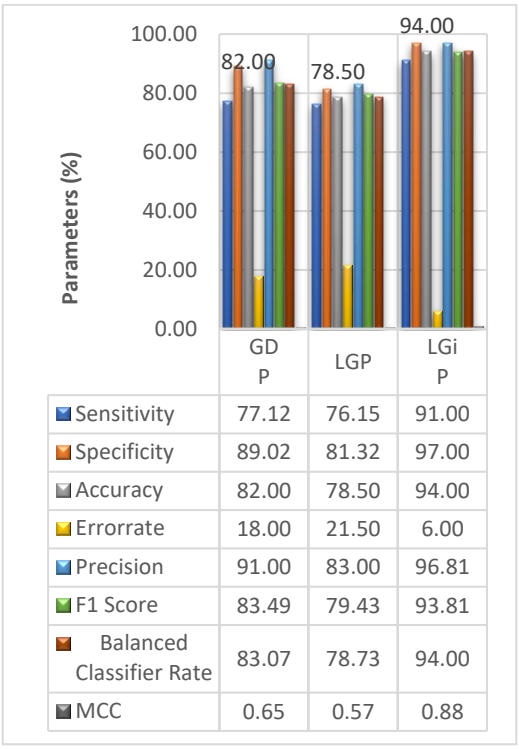

	GDP	LGP	LGiP
Sensitivity	77.12	76.15	91.00
Specificity	89.02	81.32	97.00
Accuracy	82.00	78.50	94.00
Errorrate	18.00	21.50	6.00
Precision	91.00	83.00	96.81
F1 Score	83.49	79.43	93.81
Balanced Classifier Rate	83.07	78.73	94.00
MCC	0.65	0.57	0.88

Figure 6. Performance of the classifiers

7. Conclusions

- This paper suggests method for getting optimum feature extraction technique for classify interms of parameters using CT Scan medical images. We applied the Perona-Malik second-order partial differentiation filtration method. Following this, we conducted three statistical histogram feature extraction. When comparing the classification performance of the KNN Classifier using LGP gives Lowest Accuracy is 82 and KNN Classifier with MDP gives accuracy between LGP and LGDip. Finally we found that the KNN Classifier utilizing LDiP achieved higher accuracy is 94 percentages based on standard parameters.

References

[1] Dewey, M., Siebes, M., Kachelrie, M., Kofoed, K. F., Maurovich-Horvat, P., Nikolaou, K.,&Rybicki, F. J. **(2016)**. Clinical quantitative cardiac imaging for the assessment of myocardial ischemia.Circulation: Cardiovascular Imaging, 9(6), e004101.

[2] Husmann, L., Leschka, S., Desbiolles, L., Schepis, T., Gaemperli, O., Seifert, B., ...&Alkadhi, H. **(2011)**. Coronary artery motion and cardiac phases: dependency on

heart rate—implications for CT image reconstruction. Radiology, 261(2), 582-590.

[3] Y.L., Kaveh, M.: Fourth-order partial differential equations for noise removal. IEEE Trans. ImageProcess. 9, 1723–1730 (2000)

[4] Gottschalk, A., Saeed, M., Reichek, N., &Carr, J. **(2015)**. Cost-effectiveness of cardiovascular magnetic resonance and positron emission tomography/computed tomography for selecting patients with ischemic heart disease. Journal of the American College of Cardiology, 66(11), 1352-1353.

[5] Perona, P., & Malik, J. **(1990)**. "Scale-space and edge detection using anisotropic diffusion." IEEETransactions on Pattern Analysis and Machine Intelligence, 12(7), 629-639.

[6] Sapiro, G., &Donoho, D. L. **(1995)**. "Scale invariance and noise in natural images." In Proceedings of the Royal Society of London. Series B: Biological Sciences, 259(1351), 439-445.

[7] Liu, C., Wechsler, H. **(2000)**. "Gabor Feature Based Classification Using the Enhanced Fisher LinearDiscriminant Model for Face Recognition." IEEE Transactions on Image Processing, 9(4), 650-661.

[8] Zhao, G., Pietikainen, M. **(2007)**. "Dynamic Texture Recognition Using Local Binary Patterns with anApplication to Facial Expressions." IEEE Transactions on Pattern Analysis and Machine Intelligence, 29(6), 915-928.

[9] Wang, J., Chen, Y., Hao, P., &Qian, Y. **(2012)**. "A new non-negative local density peak (NNLDP) feature extraction algorithm and its application in image recognition." Neural Computing and Applications, 21(8), 1825-1836.

[10] Kong, D., & Ma, J. (2015**)**. "Image Retrieval Based on Wavelet Transform and Second-orderGlobalDensity Peak Histogram." In Proceedings of the International Conference on Artificial Intelligence andComputer Science.

[11] Liu, Z., Lin, Z., Shan, S., & Chen, X**. (2011)**. "Learning expressionlets on spatio-temporal manifold for dynamic facial expression recognition." In IEEE Conference on Computer Vision and Pattern Recognition.

[12] Li, Y., Wang, J., & Ding, W. **(2017)**. A novel algorithm based on P-R equation and K-nearest neighbor for intrusion detection. In 2017 IEEE International Conference on Computational Science and Engineering (CSE) and IEEE International Conference on Embedded and Ubiquitous Computing (EUC) (pp. 380-385). IEEE.

[13] Yin, X., Fu, X., & Sun, G. **(2016)**.An improved KNN classification algorithm based on P-R equation.In 2016 11th International Conference on Intelligent Systems and Knowledge Engineering (ISKE) (pp. 1-4). IEEE.

[14] Zhang, Q., & Yu, H. **(2019)**. Improving KNN algorithm for high dimensional data classification based on P-R equation. In 2019 IEEE International Conference on Computational Science and Engineering (CSE) and IEEE International Conference on Embedded and Ubiquitous Computing (EUC) (pp. 158-163). IEEE.